Perturbation schemes for flow in random media

1994 J. Phys. A: Math. Gen. 27 5135

(http://iopscience.iop.org/0305-4470/27/15/014)

J. Phys. A: Math. Gen. 27 (1994) 5135–5144. Printed in the UK

Perturbation schemes for flow in random media

D S Dean, I T Drummond and R R Horgan

Department of Applied Mathematics and Theoretical Physics, University of Cambridge, Silver St, Cambridge CB3 9EW, UK

Received 22 March 1994

Abstract. We utilize a many-body style formalism to compute the long-range effective diffusivity κ_e, for dispersal of a passive scalar field in a random irrotational flow with molecular diffusivity. By comparing the theoretical results with the outcome of computer simulations we show that a renormalization-group approach that includes an appropriate vertex renormalization is superior to low-order perturbation theory and to the Hartree–Fock approximation, and gives a rather accurate method of computing κ_e for a range of parameter values.

1. Introduction

Graphical techniques for the perturbative analysis of the large-scale behaviour of fluid flow and transport in various random environments have been developed by a number of authors [1–6]. In this paper we describe an extension of these techniques [7] to the problem of a passive scalar transported by a random irrotational flow, and study the efficacy of different resummation methods by comparing the results with computer simulation. We infer the large-scale properties of the dispersal from the long-range behaviour of the ensemble average of the Green function $\langle G(\boldsymbol{x})\rangle$, where $G(\boldsymbol{x})$ is the steady-state solution for a unit point source of a contaminant at the origin. We are concerned with calculating the effective diffusivity κ_e, which is defined by

$$\langle G(\boldsymbol{x})\rangle \sim \frac{\Gamma(D/2-1)}{2\pi^{D/2}\kappa_e|\boldsymbol{x}|^{(D-2)}} \qquad \text{as} \quad |\boldsymbol{x}| \to \infty \tag{1}$$

in D dimensions.

$G(\boldsymbol{x})$ satisfies the equation

$$\kappa_0\nabla^2 G + \lambda\nabla\phi\cdot\nabla G = -\delta(\boldsymbol{x}) \tag{2}$$

where the velocity field of the random flow is $\boldsymbol{v} = \lambda\nabla\phi(\boldsymbol{x})$, and $\phi(\boldsymbol{x})$ is a random Gaussian field with zero mean. The molecular diffusivity is κ_0 which we shall subsequently set to unity for convenience.

Using graphical rules set out below, we calculate κ_e in the Hartree–Fock approximation and by exploiting renormalization-group methods.

2. Perturbation theory

We take ϕ to be homogeneous Gaussian random field characterized by

$$\langle\phi(\boldsymbol{x})\rangle = 0 \qquad \text{and} \qquad \langle\phi(\boldsymbol{x})\phi(\boldsymbol{y})\rangle = \Delta(\boldsymbol{x}-\boldsymbol{y}) \tag{3}$$

0305-4470/94/155135+10$19.50

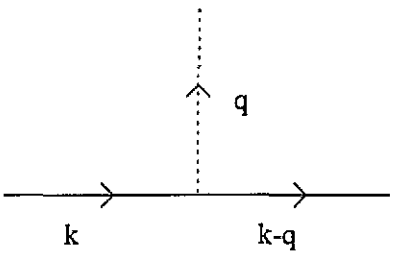

Figure 1. Vertex diagram.

the angled brackets indicating averaging over the disorder. We shall also take the disorder to be isotropic, that is $\Delta = \Delta(|x|)$. In Fourier space, equation (2) in D dimensions becomes

$$\tilde{G}(k) = \frac{1}{k^2} - \frac{\lambda}{(2\pi)^D k^2} \int \mathrm{d}q\ (k-q)\cdot q\tilde{\phi}(q)\,\tilde{G}(k-q)\ . \tag{4}$$

On iteration this expression gives the perturbation expansion of $\tilde{G}(k)$ in powers of λ. The disorder-averaged Green function is calculated using Wick's theorem and we obtain

$$\langle\tilde{G}(k)\rangle = \frac{1}{k^2 - \Sigma(k)} \tag{5}$$

where $\Sigma(k)$ denotes the one-particle-irreducible diagrams. The asymptotic (1) implies that

$$\langle\tilde{G}(k)\rangle \sim \frac{1}{\kappa_e k^2} \qquad \text{as} \quad k \to 0 \tag{6}$$

i.e. for small $|k|$, the terms in $\Sigma(k)$ of $O(k^2)$ renormalize κ_e over long distances from unity to

$$\kappa_e = 1 - \frac{\mathrm{d}}{\mathrm{d}k^2}\Sigma(k)|_{k=0}\ . \tag{7}$$

The Feynman rules for the diagrammatic perturbation expansion are as follows:

(i) Wavevector is conserved at each vertex.
(ii) Each full line carries a factor of $1/k^2$.
(iii) Wavevector is integrated around closed loops with a factor $\mathrm{d}q/(2\pi)^D$.
(iv) Each vertex of the form of figure 1 carries a factor $\lambda(k-q)\cdot q$.
(v) Each dotted line carries a factor $\tilde{\Delta}(q)$.

Applying these rules we find to $O(\lambda^4)$

$$\begin{aligned}\Sigma(k) = &-\frac{\lambda^2}{(2\pi)^D}\int \mathrm{d}q \frac{\tilde{\Delta}(q)\, q\cdot(k-q)\, q\cdot k}{(k-q)^2} \\ &+\frac{\lambda^4}{(2\pi)^{2D}}\int \mathrm{d}q\,\mathrm{d}q' \frac{\tilde{\Delta}(q)\,\tilde{\Delta}(q')\, q\cdot(k-q)\, q'\cdot(k-q-q')\, q'\cdot(k-q)\, q\cdot k}{(k-q)^4\,(k-q-q')^2} \\ &+\frac{\lambda^4}{(2\pi)^{2D}}\int \mathrm{d}q\,\mathrm{d}q' \frac{\tilde{\Delta}(q)\,\tilde{\Delta}(q')\, q\cdot(k-q)\, q'\cdot(k-q-q')\, q\cdot(k-q')\, q'\cdot k}{(k-q)^2\,(k-q')^2\,(k-q-q')^2}\ .\end{aligned}$$

To one loop we find

$$\kappa_e = 1 - \frac{\lambda^2}{D}\Delta(0)\ . \tag{8}$$

Higher-order terms can be evaluated directly using the above rules as in [5]. However, our aim is to show that properly formulated calculations at the one-loop level can account for important higher-order effects in a physically understandable way.

3. Hartree–Fock approximation

In the Hartree–Fock method $\Sigma(k)$ is approximated by the sum over 'rainbow' diagrams which we denote by $\Omega(k)$ and which are shown in figure 2.

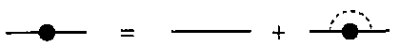

Figure 2. The rainbow diagram summation for the propagator corresponding to the Hartree–Fock approximation.

The Green function in this approximation is given by

$$\langle \tilde{G}(k) \rangle \simeq \frac{1}{k^2 - \Omega(k)}. \tag{9}$$

However, we have the self-consistency equation

$$\Omega(k) = \frac{-\lambda^2}{(2\pi)^D} \int \mathrm{d}q \, \frac{(k-q)\cdot qk \cdot q\tilde{\Delta}(q)}{(k-q)^2 - \Omega(k-q)}. \tag{10}$$

Note the linearized form of this equation gives the sum of the rainbow graphs, which look like sequences of loops stacked on loops, as can be seen from a similar style argument. After performing the angular integration, the resulting form of (10) is

$$\Omega(k) \equiv Z(k) = \frac{-\lambda^2}{16\pi^2 k^3} \int_0^\infty \mathrm{d}\Lambda \, \Lambda\tilde{\Delta}(\Lambda) \int_{|k-\Lambda|}^{k+\Lambda} \mathrm{d}q \, \frac{\left(k^2-q^2\right)^2 - \Lambda^4}{q(1-Z(q))}. \tag{11}$$

One possible form for the correlation function in three dimensions is

$$\tilde{\Delta}_2(q) = (2\pi)^{3/2} \Lambda_0^{-3} \exp\left(-\frac{q^2}{2\Lambda_0^2}\right). \tag{12}$$

(Note that normalizations are chosen in accordance with the convention $\Delta(0) = 1$.) In the correlation functions above, we see that there is only one length scale introduced, i.e. Λ_0^{-1}. Therefore, by dimensional analysis, Z is a function of k/Λ_0 and we can, without loss of generality, take $\Lambda_0 = 1$. We may solve (11) numerically, and the fact that the Hartree–Fock approximation can be thought of as being obtained from successive iterations of rainbow graphs suggests that an iterative numerical scheme would be successful. The Gaussian form of the two-point correlation function (12) means that one can terminate the range of integration quite quickly—when $\Lambda_0 = 1$ the cut-off was taken to be at $k = 20$. The explicit form of the equation in this case is

$$Z(k) = -\frac{\lambda^2}{(2\pi)^{1/2}} \int_0^\infty \mathrm{d}q \, \frac{\mathrm{e}^{-1/2\left(k^2+q^2\right)}}{qk^3(1-Z(q))} R(k,q) \tag{13}$$

where

$$R(k,q) = \left[2\left(k^2+q^2\right)(kq\cosh(kq) - \sinh(kq)) - 4\left(\left(k^2q^2+1\right)\sinh(kq) - kq\cosh(kq)\right)\right]. \tag{14}$$

The iterations converged after about ten steps and the dependence of the solution on the step size chosen did not vary significantly on going from 0.05 to 0.02 (i.e. 400 grid points to 1000 grid points). The linearized form of the Hartree–Fock equation was also solved. For values of λ slightly greater than unity the iterations did not converge (the value at which this happened was 1.0443, but one would need greater confidence in the numerical techniques used before making a definitive statement), and the linearized form of the equation yielded values for $Z(0)$ greater than 1 and hence negative diffusivities.

4. One-loop renormalization-group analysis

The most straightforward formulation of the renormalization-group method is to split the field ϕ into two components $\phi_\Lambda^>$ and $\phi_\Lambda^<$, where

$$\phi_\Lambda^>(x) = \frac{1}{(2\pi)^D}\int_{|q|>\Lambda} \mathrm{d}q\, \mathrm{e}^{\mathrm{i}q\cdot x}\tilde{\phi}(q) \tag{15}$$

and

$$\phi_\Lambda^<(x) = \frac{1}{(2\pi)^D}\int_{|q|<\Lambda} \mathrm{d}q\, \mathrm{e}^{\mathrm{i}q\cdot x}\tilde{\phi}(q)\,. \tag{16}$$

This is equivalent to the approach used in [8]. The assumption made is that the high-wavenumber behaviour can be averaged out to yield a renormalized form of (2), namely

$$\kappa(\Lambda)\nabla^2 G_\Lambda + \lambda\nabla\phi_\Lambda^<\cdot\nabla G_\Lambda = -\delta(x) \tag{17}$$

where the deviation from unity of the renormalized diffusivity $\kappa(\Lambda)$, is due to the high-wavenumber component ($\phi_\Lambda^>$) of the random field ϕ, and G_Λ is the Green function for the system after this high-wavenumber component of the field has been averaged out. In principle, the equation satisfied by G_Λ is more complex than (17) since the averaging procedure generates new terms linear in G_Λ that are higher order in numbers of derivatives and powers of ϕ_Λ than those included. The approximation we adopt is to neglect these new terms. The next step is to average out a further component of the field ϕ that has support on the infinitesimal shell of wavenumber space $|q| \in (\Lambda, \Lambda - \delta\Lambda)$, and then see how this modifies $\kappa(\Lambda)$.

From equation (7) we know that

$$\kappa(\Lambda) = 1 - \frac{\mathrm{d}}{\mathrm{d}k^2}\Sigma_\Lambda(k)\,|_{k=0} \tag{18}$$

where $\Sigma_\Lambda(k)$ indicates the one-particle-irreducible diagrams evaluated with the low-wavenumber cut-off Λ. If we now average out the shell of width $\delta\Lambda$ then to $O(\delta\Lambda)$, which is simply the one-loop contribution, we find

$$\Sigma_{\Lambda-\delta\Lambda}(k) = \Sigma_\Lambda(k) - \frac{\lambda^2}{(2\pi)^D}\int_{\Lambda-\delta\Lambda<|q|<\Lambda} \mathrm{d}q\, \frac{\tilde{\Delta}(q)\, q\cdot(k-q)\, q\cdot k}{\kappa(\Lambda)(k-q)^2}\,. \tag{19}$$

The factor $\kappa(\Lambda)$ appears in the denominator of the integrand as we have assumed that we have started with (17). Hence we find

$$\Sigma_{\Lambda-\delta\Lambda}(k) - \Sigma_\Lambda(k) = \frac{\lambda^2}{(2\pi)^D D\kappa(\Lambda)} k^2 S_D \Lambda^{D-1}\tilde{\Delta}(\Lambda)\,\delta\Lambda + o\left(k^2\delta\Lambda\right) \tag{20}$$

where S_D is the surface area of the unit $D-1$ sphere. Using (18) we find

$$\frac{\mathrm{d}\kappa(\Lambda)}{\mathrm{d}\Lambda} = \frac{\lambda^2}{(2\pi)^D D\kappa(\Lambda)} S_D \Lambda^{D-1}\tilde{\Delta}(\Lambda)\,. \tag{21}$$

Therefore in this scheme of approximation the effective diffusivity is given by

$$\kappa_e = \kappa(0) = \left(1 - \frac{2\lambda^2}{D(2\pi)^D} S_D \int_0^\infty \mathrm{d}\Lambda'\, \Lambda'^{D-1}\tilde{\Delta}(\Lambda')\right)^{1/2} \tag{22}$$

$$= \left(1 - \frac{2}{D}\lambda^2\Delta(0)\right)^{1/2}. \tag{23}$$

This result is, of course, consistent with first-order perturbation theory.

5. Improved renormalization

In this section we improve the renormalization-group scheme by including the vertex correction which causes λ to be renormalized in a way dependent on the scale Λ. We denote the running value of this coupling by $\lambda(\Lambda)$, where $\lambda(\infty) = \lambda$. The interaction vertex shown in figure 1 can be associated with a tensor Γ_{ij}, the value of the vertex being given by

$$\Gamma_{ij} q^i (k-q)^j . \tag{24}$$

Before renormalization, i.e. in the bare system,

$$\Gamma_{ij} = \lambda \delta_{ij} \tag{25}$$

the self-similarity ansatz says that we only keep vertex interactions of this form, this amounts to insisting that the renormalized random field remains Gaussian. Carrying out a partial averaging in wavenumber space, and averaging out the Fourier modes of the random field in the infinitesimal shell in wavenumber space $(\Lambda - \delta\Lambda, \Lambda)$, we introduce a new interaction shown diagrammatically in figure 3. This diagram is equal to

$$-\left[\frac{\lambda^3(\Lambda)}{(2\pi)^D \kappa^2(\Lambda)} \int_{\Lambda-\delta\Lambda<|q'|<\Lambda} \mathrm{d}q' \, \tilde{\Delta}(q') \frac{(k-q')\cdot q' (k-q-q')^i q'^j}{(k-q')^2 (k-q-q')^2}\right] q^i (k-q)^j$$
$$= \delta\Gamma_{ij}(k,q) q^i (k-q)^j . \tag{26}$$

The self-similarity ansatz tells us to neglect any higher-order terms in k and q and thus we approximate $\delta\Gamma_{ij}(k,q)$ by $\delta\Gamma_{ij}(0,0)$ (one could also argue that this is valid because the long-range interactions, i.e. the low-wavenumber regime, make the dominant contributions). Hence

$$\delta\Gamma_{ij} \approx -\frac{\lambda^3(\Lambda)}{(2\pi)^D \kappa^2(\Lambda)} \int_{|q'|=\Lambda} \mathrm{d}q' \, \tilde{\Delta}(q') \frac{q'^i q'^j}{q'^2} \delta\Lambda \tag{27}$$

$$= -\delta_{ij} \frac{\lambda^3(\Lambda)}{(2\pi)^D D\kappa^2(\Lambda)} S_D \Lambda^{D-1} \tilde{\Delta}(\Lambda) \delta\Lambda . \tag{28}$$

Consequently, comparing (28) with (25), we find

$$\lambda(\Lambda - \delta\Lambda) = \lambda(\Lambda) - \frac{\lambda^3(\Lambda)}{(2\pi)^D D\kappa^2(\Lambda)} S_D \Lambda^{D-1} \tilde{\Delta}(\Lambda) \delta\Lambda \tag{29}$$

and hence

$$\frac{\mathrm{d}\lambda(\Lambda)}{\mathrm{d}\Lambda} = \frac{\lambda^3(\Lambda)}{(2\pi)^D D\kappa^2(\Lambda)} S_D \Lambda^{D-1} \tilde{\Delta}(\Lambda) . \tag{30}$$

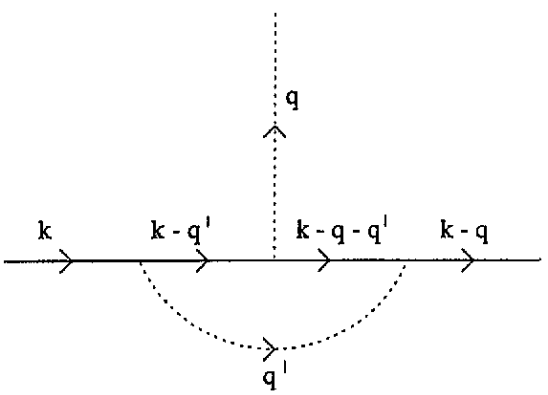

Figure 3. Renormalized vertex.

In this scheme the renormalization-group flow occurs in a two-dimensional space $(\kappa(\Lambda), \lambda(\Lambda))$ and the equation describing the flow of $\kappa(\Lambda)$ is modified from (21) to

$$\frac{\mathrm{d}\kappa(\Lambda)}{\mathrm{d}\Lambda} = \frac{\lambda^2(\Lambda)}{(2\pi)^D D\kappa(\Lambda)} S_D \Lambda^{D-1} \tilde{\Delta}(\Lambda) \tag{31}$$

as we must use the running value of λ when we renormalize $\kappa(\Lambda)$. Therefore the renormalization-group equation for $\kappa(\Lambda)$ is

$$\frac{\mathrm{d}\kappa(\Lambda)}{\mathrm{d}\Lambda} = \frac{\lambda^2\kappa(\Lambda)}{(2\pi)^D D} S_D \Lambda^{D-1} \tilde{\Delta}(\Lambda) \tag{32}$$

and hence the estimate for κ_e under this scheme is

$$\kappa_e = \kappa(0) = \exp\left(-\frac{\lambda^2 \Delta(0)}{D}\right). \tag{33}$$

6. The numerical simulation

The simulation is based on the numerical integration of the relevant stochastic differential equation for a large number of particles in a large number of realizations of the flow field. We are interested in the calculation of the inverse of the operator

$$H = \nabla^2 + \lambda \nabla\phi \cdot \nabla. \tag{34}$$

The operator H is the generator for the diffusion obeying the stochastic differential equation

$$\mathrm{d}\boldsymbol{X}_t = \sqrt{2}\,\mathrm{d}\boldsymbol{B}_t + \lambda \nabla\phi(\boldsymbol{X}_t)\,\mathrm{d}t. \tag{35}$$

A naive discretization for the stochastic differential equation (35) is

$$\Delta\boldsymbol{x} = (2\Delta t)^{1/2}\boldsymbol{\xi} + \lambda \nabla\phi(\boldsymbol{x})\,\Delta t \tag{36}$$

where the components of $\boldsymbol{\xi}$ are independent $N(0, 1)$ random variables. However, when implemented, the above algorithm yields a probability distribution which evolves with an error $O(\Delta t)$. It is therefore better to use the extended Runge–Kutta scheme [2, 9]:

$$\Delta\boldsymbol{x} = (\Delta t)^{1/2}(\boldsymbol{\xi}_1 + \boldsymbol{\xi}_2) + \lambda \nabla\phi(\boldsymbol{x}')\,\Delta t \tag{37}$$

where

$$\boldsymbol{x}' = \boldsymbol{x} + \tfrac{1}{2}\lambda \Delta t \nabla\phi(\boldsymbol{x}) + (\Delta t)^{1/2}\boldsymbol{\xi}_1 \tag{38}$$

and $\boldsymbol{\xi}_1$ and $\boldsymbol{\xi}_2$ are independent random vectors whose components are $N(0, 1)$. This extended algorithm generates a probability distribution evolving with error $O((\Delta t)^2)$.

The realizations of the random field are constructed by a method which is a simplification of that introduced in [10] and which was used in [5]. We set

$$\phi(\boldsymbol{x}) = \left(\frac{2}{N}\right)^{1/2} \sum_{n=1}^{N} \cos(\boldsymbol{k}_n \cdot \boldsymbol{x} + \epsilon_n) \tag{39}$$

where $\{\epsilon_n\}$ and $\{\boldsymbol{k}_n\}$ are independently distributed random variables. Each phase ϵ_n is uniformly distributed on $[0, 2\pi]$. If $P(\boldsymbol{k})$ denotes the probability distribution for the $\boldsymbol{k}_n$, then one finds

$$\langle\phi(\boldsymbol{x})\phi(\boldsymbol{y})\rangle = \int \mathrm{d}\boldsymbol{k}\, P(\boldsymbol{k}) \cos(\boldsymbol{k} \cdot (\boldsymbol{x} - \boldsymbol{y})). \tag{40}$$

Consequently to obtain the correlation function required we choose $P(\boldsymbol{k})$ to be the Fourier transform of Δ. By the central limit theorem the field ϕ converges to a Gaussian as the

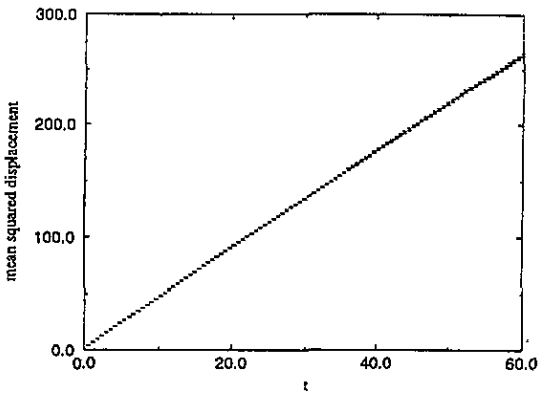

Figure 4. Simulated mean squared displacement against time for $\lambda = 1$.

number of modes N is increased, the deviations from Gaussian statistics being of order $1/N$. In our simulation N is taken to be 128. In order for comparison with the theoretical results and for computational simplicity, we take

$$P(k) = \frac{1}{(2\pi)^{3/2}} e^{-k^2/2} \tag{41}$$

i.e. we choose each of the components of the k_n to be $N(0, 1)$.

The basis of the simulation is to track the trajectories of particles in M realizations of the field ϕ, each realization of the field containing N modes: M and N are taken to be 256 and 128, respectively, and the number of particles tracked in each realization is also taken to be N. The particles in each realization are started two correlation lengths apart (in our case a distance of 2) in order to take full advantage of any decorrelation within individual realizations. The average of some quantity g is calculated from within individual realizations by averaging over particle paths to give estimators $\langle g \rangle_i$, $1 \leqslant i \leqslant M$, and the final estimator $\langle g \rangle$ and its variance are computed by the standard mini-ensemble formulae

$$\langle g \rangle = \frac{1}{M} \sum_{n=1}^{M} \langle g \rangle_i \tag{42}$$

and

$$\sigma_g^2 = \frac{1}{M-1} \sum_{n=1}^{M} \left(\langle g \rangle_i^2 - \langle g \rangle^2 \right) . \tag{43}$$

The assumption that an effective diffusivity exists implies that

$$\left\langle E\left(X_t^2\right) \right\rangle \sim 2D\kappa_e t \tag{44}$$

for sufficiently large t. Noting this we may measure κ_e in two ways.

(i) The mean squared displacement is measured in the simulation and its average plotted against time. The asymptotic slope is used to calculate the effective diffusivity. The simulation is run for a total of 60 s (600 time steps of length 0.1), as we can see from figure 4 the graph becomes linear reasonably quickly. In order to ensure we are sampling the asymptotic slope only the final 30 s of data was used. The slope of this data is estimated using a least-squares fit.

(ii) Applying Ito's formula [11] and using the stochastic differential equation (35) we find

$$\mathrm{d}X_t^2 = 2X_t \cdot \mathrm{d}X_t + (\mathrm{d}X_t)^2 \tag{45}$$

$$= 2X_t \cdot (\sqrt{2}\mathrm{d}B_t + \lambda \nabla\phi(X_t)) + 2\,\mathrm{d}t . \tag{46}$$

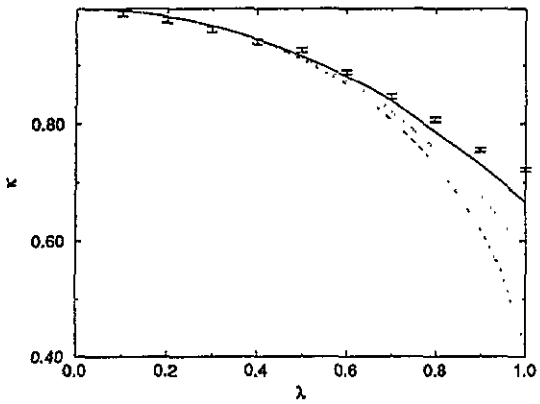

Figure 5. Results for κ_e using measurement method (i) shown with one-loop perturbation theory (full curve), one-loop renormalization group (dotted curve) and Hartree–Fock (broken curve).

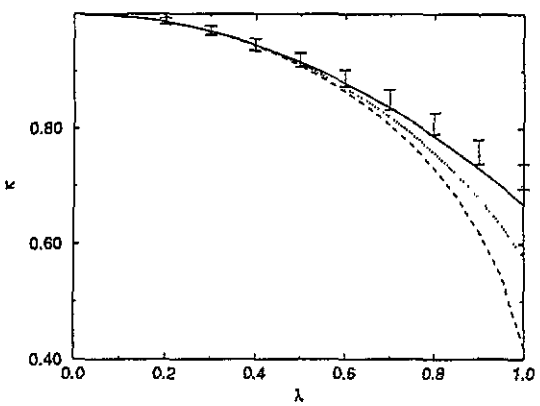

Figure 6. Results for κ_e using measurement method (ii) shown with one-loop perturbation theory (full curve), one-loop renormalization group (dotted curve) and Hartree–Fock (broken curve).

Taking expectations we obtain

$$\frac{\mathrm{d}}{\mathrm{d}t}E\left(\boldsymbol{X}_t^2\right) = 2D + 2\lambda E\left(\boldsymbol{X}_t \cdot \nabla\phi\left(\boldsymbol{X}_t\right)\right) . \tag{47}$$

Hence another estimator for κ_e is given by the asymptotic value of

$$\kappa(t) = 1 + \frac{\lambda}{D}\langle E\left(\boldsymbol{X}_t \cdot \nabla\phi\left(\boldsymbol{X}_t\right)\right)\rangle . \tag{48}$$

In estimating κ_e from this data we weight in favour of data points with smaller standard deviations in the usual way, that is we take

$$\kappa_e = \frac{\sum \kappa_i \sigma_i^{-1}}{\sum \sigma_i^{-1}} . \tag{49}$$

The standard error on the estimate of κ_e is taken to be the maximum standard deviation from the points in the data used, i.e. $\max(\sigma_i)$. This is a very conservative estimate of the error. In addition any decorrelation over time of the measured data would also reduce the quoted error. The results for measurements (i) and (ii) for the range $0 < \lambda < 1$ are shown plotted in figures 5 and 6, respectively, together with the predicted values from one-loop perturbation theory, one-loop renormalization-group analysis and the Hartree–Fock approximation. The results of the full self-similar renormalization-group analysis against results from measurement types (i) and (ii) are shown in figures 7 and 8, respectively, for the range $0 < \lambda < 2$.

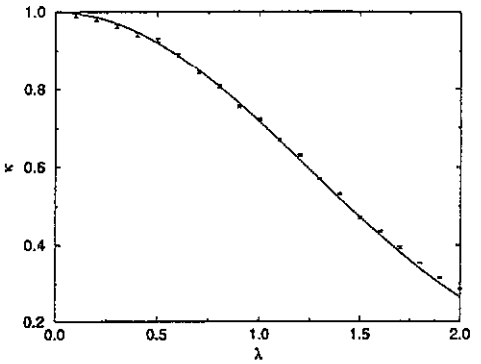

Figure 7. Results for κ_e using measurement method (i) shown with predictions of self-similar renormalization-group analysis.

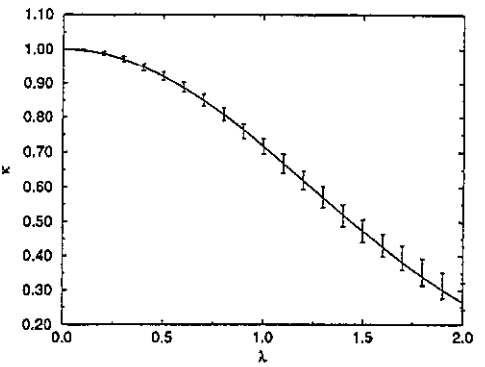

Figure 8. Results for κ_e using measurement method (ii) shown with predictions of self-similar renormalization-group analysis.

7. Discussion and conclusions

The simple one-loop perturbation theory gives a reasonable prediction for κ_e up to $\lambda \sim \frac{1}{2}$, but predicts too small a value for larger values of λ. Both the Hartree–Fock and the simplest one-loop renormalization-group methods actually perform worse than basic one-loop perturbation theory, predicting results that are even lower for the larger values of λ. This is evident from figures 5 and 6. In contrast, the self-similar renormalization-group method performs very well over an even larger range of λ, as is shown in figures 7 and 8. We attribute the success of the self-similar method to the incorporation of new interactions in the form of a vertex renormalization and to the fact that a full self-similarity assumption is a natural one to make since we believe that the physical picture is not drastically altered by renormalization. The outcome is to give a result that is independent of the details of the spectrum and depends only on $\Delta(0)$: the integral over the wavenumber spectrum.

We remark that the use of the diagrammatic method makes it easy to identify the inclusion of coupling constant renormalization as a natural way to improve the renormalization-group calculation. In principle, further improvements can be made in a systematic way by including new couplings generated by higher loop effects which are associated with new terms in the equation for the Green function. The importance of these higher-order effects, especially at larger values of λ, remains to be investigated.

In the absence of molecular diffusivity ($\kappa_0 = 0$) all particles in a time-independent gradient flow will accumulate at local maxima of $\phi(x)$. This implies that $\kappa_e = 0$ when either ($\kappa_0 = 0$) or $\lambda \to \infty$ for fixed κ_0. Only the improved renormalization-group calculation of κ_e has these properties. This gives confidence that this method is a physically sensible scheme and is likely to give good results when applied to more general models than that discussed in this paper.

Acknowledgment

This work was completed with the support from EU grant CHRX-CT93-0411.

References

[1] Phythian R and Curtis W D 1978 The effective long-time diffusivity for a passive scalar field in a Gaussian flow *J. Fluid Mech.* **89** 241

[2] Drummond I T, Duane S and Horgan R R 1984 Scalar diffusion in simulated helical turbulence with molecular diffusivity *J. Fluid Mech.* **138** 75–91

[3] Drummond I T and Horgan R R 1986 Numerical simulation of the α-effect and turbulent magnetic diffusion with molecular diffusivity *J. Fluid Mech.* **163** 425–38

[4] King P R 1987 The use of field theoretic methods for the study of flow in a heterogenous porous medium *J. Phys. A: Math. Gen.* **20** 3935–47

[5] Drummond I T and Horgan R R 1987 The effective permeability of a random medium *J. Phys. A: Math. Gen.* **20** 4661–72

[6] Drummond I T and Horgan R R 1989 Pressure fluctuations in a randomly permeable medium *J. Phys. A: Math. Gen.* **22** 3205–12

[7] Dean D S 1993 Stochastic dynamics *PhD Thesis* University of Cambridge

[8] Moffat H K 1983 Transport effects associated with turbulence, with particular attention to the influence of helicity *Rep. Prog. Phys.* **46** 621–64

[9] Drummond I T, Hoch A and Horgan R R 1986 Numerical integration of stochastic differential equations with variable diffusivity *J. Phys. A: Math. Gen.* **19** 3871–81

[10] Kraichnan R H 1976 Diffusion of passive-scalar and magnetic fields by turbulence *J. Fluid Mech.* **77** 753–68

[11] Oksendal B 1989 *Stochasic Differential Equations* (Berlin: Springer)